nature nanotechnology

REVIEW ARTICLE

PUBLISHED ONLINE: 6 DECEMBER 2009 | DOI: 10.1038/NNANO.2009.347

Atomic force microscopy as a tool for atom manipulation

Oscar Custance[1]*, Ruben Perez[2] and Seizo Morita[3]

During the past 20 years, the manipulation of atoms and molecules at surfaces has allowed the construction and characterization of model systems that could, potentially, act as building blocks for future nanoscale devices. The majority of these experiments were performed with scanning tunnelling microscopy at cryogenic temperatures. Recently, it has been shown that another scanning probe technique, the atomic force microscope, is capable of positioning single atoms even at room temperature. Here, we review progress in the manipulation of atoms and molecules with the atomic force microscope, and discuss the new opportunities presented by this technique.

At the beginning of 1990, while many groups worldwide were still trying to achieve atomic resolution with the scanning tunnelling microscope[1] (STM), researchers at IBM astounded the scientific community by positioning 35 xenon atoms on a nickel(110) surface to spell out the company logo[2]. The following year researchers, again from IBM, demonstrated the capability of the STM to vertically manipulate atoms of semiconductor surfaces[3] and, more importantly, to reversibly transfer a single atom between the tip of a STM and a metallic surface — which leads to switching behaviour in the tunnelling current — by applying an appropriate voltage bias[4]. These pioneering experiments inspired visions of devices based on just a few atoms or molecules but, despite the efforts of many researchers, there have only been a few demonstrations of real devices and instruments controlled by the movement of just a few atoms[5].

In the course of developing the technology needed to create atomic and molecular machines, the STM has been used to construct and study model systems to learn more about the behaviour, properties and possible functionality of the building blocks for future nanoscale devices. Significant achievements in this direction include, among others, observing the initial formation of an atomic wire[6], studying the influence of the contact between an electrode and a single molecule on the properties of single-molecule devices[7–9], and computation with individual molecules[10]. The STM has also been extensively used to study, among other phenomena, the quantum confinement of electrons in two[11–13] and three dimensions[14], the implantation of single atomic dopants at surfaces[15], the doping of single molecules[16], the stimulation of chemical reactions with atomic-scale precision[17], conformational changes of molecules at surfaces[18–22], single bonds[23] and the magnetic properties of structures designed at the atomic scale[24–25]. In all of these studies the capability of the STM to manipulate atoms and molecules was crucial.

The development of new operating modes[26–28] for the atomic force microscope[29] (AFM) in recent years has made it possible to image the surfaces of both conducting and insulating bulk materials with true atomic-scale resolution, and also to manipulate single atoms and molecules. Although still in its infancy, atom manipulation with the AFM has demonstrated tremendous potential for exploring the fundamental properties of matter at the nanoscale.

In this review, we present a summary of the progress made so far in atom manipulation using the AFM, and discuss the opportunities that this technique may bring to the control and study of artificial structures engineered with atomic precision.

Basics of atomic-scale imaging and manipulation

Although the invention and first implementation of the STM and the AFM were relatively close in time[30], the development of their atomic resolution and atom manipulation capabilities has been at very different paces. Whereas the first atomic resolution image of a reactive surface taken with an STM was obtained soon after its invention[31], it took almost nine years for the AFM to accomplish an equally decisive result[32]; and from that point, another ten years were required to build an atomic pattern by manipulating individual atoms with an AFM[33]. This time lag is primarily due to a higher degree of instrumental complexity in atomic-resolution AFM with respect to STM that ultimately originates from the different nature of the physical observables responsible for atomic contrast in each of these techniques.

In STM, atomic resolution is possible by detecting a current of electrons quantum-mechanically tunnelling through the vacuum gap between a voltage-biased metallic tip and a conductive surface. This tunnelling current is of the order of pico- to nanoamperes (values that can be easily measured with conventional electronic techniques), and has a monotonic exponential dependence on the tip–surface separation. This dependence accounts for strong changes in the current signal on atomic-scale variations of the surface topography (typically a factor of ten per ångström in the direction perpendicular to the surface), and it ensures that the detection of the tunnelling current is mostly confined to the foremost atom of the tip. However, the detected current in STM is also essentially related to the local density of electronic states of both tip and surface, integrated over an energy window $E_F + eV_s$ where E_F represents the Fermi level (the highest occupied electron energy level), V_s is the bias voltage applied between tip and sample and e is the electron charge[34]. Thus, atomic-scale STM images are ultimately the result of a convolution of the surface topography and the electronic structure of both tip and surface.

In AFM, atomic resolution is based on detecting the forces ascribed to the onset of the short-range bonding interaction between the foremost atom of a sharp tip at the end of a cantilever and the atoms at the surface[35–38]. These interatomic forces are of the order of pico- to nanonewtons, and they start being appreciable at a separation distance between the closest tip and surface atoms typically shorter

[1]National Institute for Materials Science, 1-2-1 Sengen, 305-0047 Tsukuba, Ibaraki, Japan, [2]Departamento de Física Teórica de la Materia Condensada, Universidad Autónoma de Madrid, 28049 Madrid, Spain, [3]Graduate School of Engineering, Osaka University, 2-1 Yamada-Oka, 565-0871 Suita, Osaka, Japan. *e-mail: custance.oscar@nims.go.jp

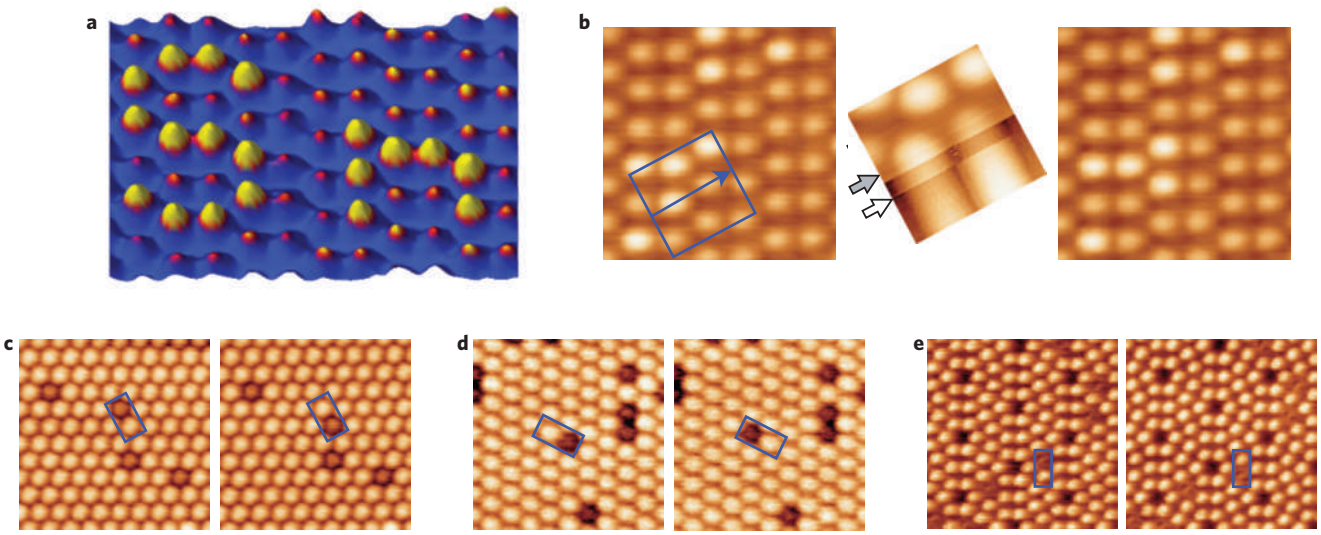

Figure 1 | Lateral-interchange atomic manipulation with an AFM. a, Atomic design created at room temperature by producing the concerted lateral interchange between substitutional Sn atoms (higher protrusions) and Ge atoms populating the Ge(111)-c(2 x 8) surface[33]. **b**, Summary of the process to manipulate these atoms. The fast-scan direction is oriented parallel to a line connecting the centre of the atoms (blue square and arrow), and the slow scan is stopped over it (grey arrow). The control of the energy barriers between adjacent adsorption sites with the AFM tip leads to the atomic interchange (white arrow)[33]. Identical protocol has been successfully applied in other surfaces[52] of very different structure and composition, such as Sn/Si(111)-($\sqrt{3} \times \sqrt{3}$)R30° (**c**), In/Si(111)-($\sqrt{3} \times \sqrt{3}$)R30° (**d**), and Sb/Si(111)-(7 × 7) (**e**), pointing towards the generality of the manipulation method.

than 5 Å. These short-range interatomic forces are detected, and very precisely quantified, by operating the AFM in dynamic mode under the frequency-modulation detection method[39] (FM-AFM). In this operation scheme, the cantilever is oscillated at resonance while keeping the oscillation amplitude constant, and the forces acting on the AFM tip are detected as changes in the cantilever resonant frequency[39]. In contrast to the STM, where the tunnelling current does not combine with other observables, the tip–surface interatomic forces responsible for atomic contrast in AFM cumulate with additional tip–surface interactions spanning over a longer distance range. In vacuum, these long-range forces correspond to the van der Waals force, the electrostatic force, and magnetic-dipole interactions[26,40]. If the magnitude of these long-range forces is significant at the closest tip–surface distances, it can seriously hamper atomic resolution by either blurring the short-range interaction or by causing the tip to come into contact with the surface[26,41]. The necessity for utmost control of the distance between the foremost atom of the oscillating tip and the surface atoms, under the ubiquitous presence of these long-range forces, has compelled the FM-AFM community to develop sophisticated instrumentation and experimental protocols over the years for sensing the tiny interatomic forces that produce atomic contrast[27,28].

The intrinsic differences in the signal detection and the operation of these two scanning probe techniques have implications regarding atom manipulation. The STM, for instance, can make use of intense electric fields between the tip and surface during bias-voltage pulses to evaporate single atoms[3] and hence create atomic-scale patterns[42]. In atomic-resolution AFM, on the other hand, the long-range electrostatic interaction is usually minimized by measuring and compensating for the tip–surface-contact potential difference[40] to get the highest sensitivity possible for the tip–surface short-range interaction. In the case of lateral manipulation of atoms with the STM, the magnitude and direction of the tip–adsorbate chemical binding force that leads to the atom movement can be tuned by respectively adjusting the vertical and lateral position of the tip above the adsorbate being manipulated[2,43]. Lateral atomic manipulation with the AFM is performed in a similar way, with the variation that the AFM tip constantly oscillates at every position over the surface with a frequency ranging from 10^3 to 10^6 Hz and a total amplitude varying from half an ångström to tens of nanometres, depending on the FM-AFM experimental set-up. Despite this dynamic movement of the probe, well-regulated cantilever dynamics during the oscillation and a high sensitivity to the tip–surface interatomic forces hold the key to fine-tuning the interactions that lead to atom manipulation. For the STM, three types of lateral atomic manipulation mechanisms have been identified, depending on the tip–surface separation: pulling, pushing and sliding[44]. The first two mechanisms have been confirmed for the AFM too, whereas the sliding mechanism is impracticable for cantilever-oscillation amplitudes larger than a few tenths of an ångström.

Preliminaries of atom manipulation with the AFM

The first reported evidence of atom manipulation using an AFM emulates one of the pioneering achievements[3] of the STM. Instead of using field evaporation to remove atoms from the Si(111)-(7 × 7) surface[3], Oyabu and co-workers[45] demonstrated that it is possible to selectively remove either a corner or central adatom of the (7 × 7) reconstruction by successively approaching the oscillating AFM tip towards the surface over the corresponding atomic position. Furthermore, by applying exactly the same protocol, they showed that an atom from the AFM tip apex could be deposited on a previously created atomic vacancy[45].

The same authors reproduced identical vertical manipulations on the Ge(111)-c(2 × 8) surface. As a consequence of these manipulations, sometimes the deposition of an adsorbate from the tip apex was obtained[46]. Oyabu and co-workers noticed that these adsorbates could be moved along the rows extending over the <1$\bar{1}$0> crystallographic direction of the Ge(111)-c(2 × 8) surface just by simply raster scanning[46], this being the first evidence that adsorbates of typical atomic dimensions could be laterally manipulated on top of a surface with an AFM. Trying to generate adsorbates in a controlled way to further explore the manipulation capabilities of the AFM, they were able to produce the displacement of individual Ge atoms from their natural adsorption positions to metastable sites with the AFM tip, and then induce their movement at the surface in processes involving the correlated displacement of more than one Ge atom[46]. Interestingly, in

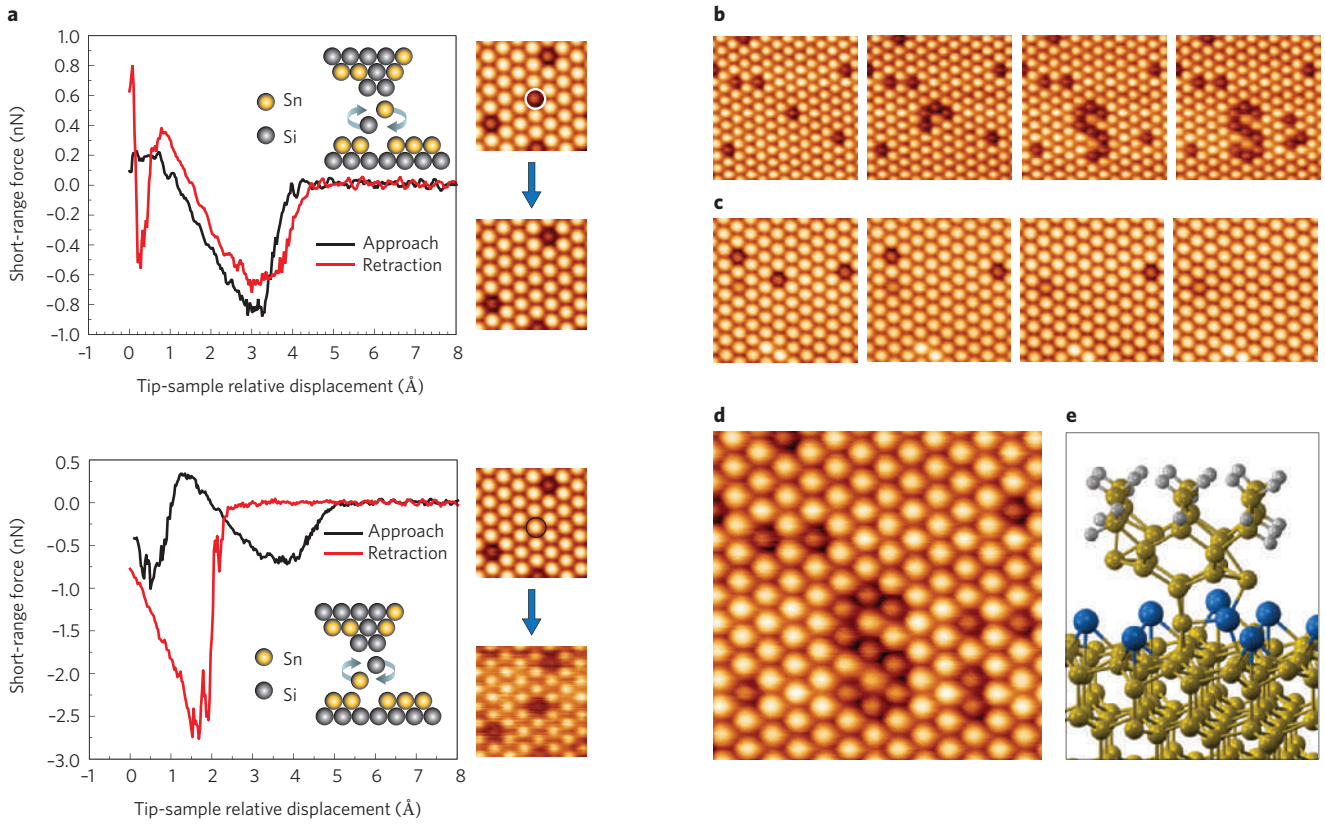

Figure 2 | Vertical-interchange atomic manipulation. a, By gently exploring the repulsive forces of the bonding interaction between the foremost atom of the AFM tip and atoms probed at a surface, it is possible to induce the vertical interchange of the interacting atoms[56]. Here, a Si defect of the Sn/Si(111)-($\sqrt{3} \times \sqrt{3}$)R30° surface (white circle) was replaced by a Sn atom coming from the AFM tip. In a subsequent process, the newly deposited Sn atom (dark circle) was substituted by a Si atom coming from the tip. Applying this manipulation method in heterogeneous semiconductor surfaces enables one to 'write' (**b**) and 'erase' (**c**) atomic markers by respectively depositing and removing the atoms in lower concentration (Si in the case of **b** and **c**). Reproducibility of this manipulation method provides another way to create atomic designs on surfaces with an AFM at room temperature (**d**). These vertical-interchange manipulations involve complex multi-atom contacts between tip and surface[56] (**e**). In **e**, silicon, tin and hydrogen atoms are represented by yellow, blue and white spheres, respectively, and the tip apex and surface models correspond to the atomic arrangements in the upper and lower halves respectively.

these atomic displacements, the surface atoms have to overcome an energy barrier of the order of ~0.8 eV (ref. 47), assisted by the interaction with the AFM tip.

These preliminary experiments on semiconductor surfaces, together with timely theoretical predictions[48,49], provided evidence for the potential of the AFM not only to produce the manipulation of single atoms and molecules weakly physisorbed on top of a surface, but also for the manipulation of strongly chemisorbed atoms. In particular, the fact that the presence of the AFM tip can locally modify the surface potential landscape so that atoms are able to overcome energy barriers close to 1 eV even at low temperatures[45,46] was an important clue to unique manipulation methods that allow the creation of stable atomic patterns with the AFM at room temperature.

Atomic patterning with the AFM

Most of the atomic and molecular designs involving complex positioning of adsorbates with the STM have been accomplished at cryogenic temperatures[2,6,10–14,50], where diffusion is hampered and the adsorbates bind at stable positions, remaining there long enough to construct the artificial pattern. Only very exceptional cases of complex molecular assemblies at room temperature have been reported[51]. In this sense, the first conclusive proof that the AFM could be used for the manipulation of individual atoms and the purposeful creation of atomic structures at surfaces[33] was doubly significant, as these atomic designs were produced at room temperature and remained stable at the surface for relatively long periods of time.

Figure 1a shows the first atomic pattern created with an AFM by laterally manipulating individual atoms at a surface[33]. These atomic manipulations are based on inducing the in-plane concerted interchange of Sn atoms (brighter protrusions in Fig. 1a,b) with the adjacent Ge atoms populating the Ge(111)-c(2 × 8) surface[33]. The Sn atoms are embedded in the surface plane by substituting some of the original Ge atoms, and therefore they are strongly bound to the underlaying atomic plane. The controlled manipulation of these Sn atoms was produced by creating a directional driving force with the AFM tip. This was done by executing successive line scans over the line connecting the centre position of two neighbouring atoms, and setting the scan direction from the Sn to the Ge atom, lifting the tip up ~1 Å on the way back. During the realization of these line scans, tip and sample were successively brought to a closer separation until it exceeded the threshold tip–surface interaction that produces the in-plane concerted atomic interchange[33] (Fig. 1b). These lateral-interchange atomic manipulations have been reproduced — also at room temperature and using an identical protocol — in other semiconductor surfaces[52] such as the ($\sqrt{3} \times \sqrt{3}$)R30° surfaces of Sn on Si(111) and In on Si(111), as well as substitutional Sb atoms at the Si(111)-(7 × 7) surface (Fig. 1c–e). These results point to a common manipulation mechanism for all these structurally different surfaces, where the manipulated atoms (donors and acceptors) were strongly bound to the underlaying atomic layer.

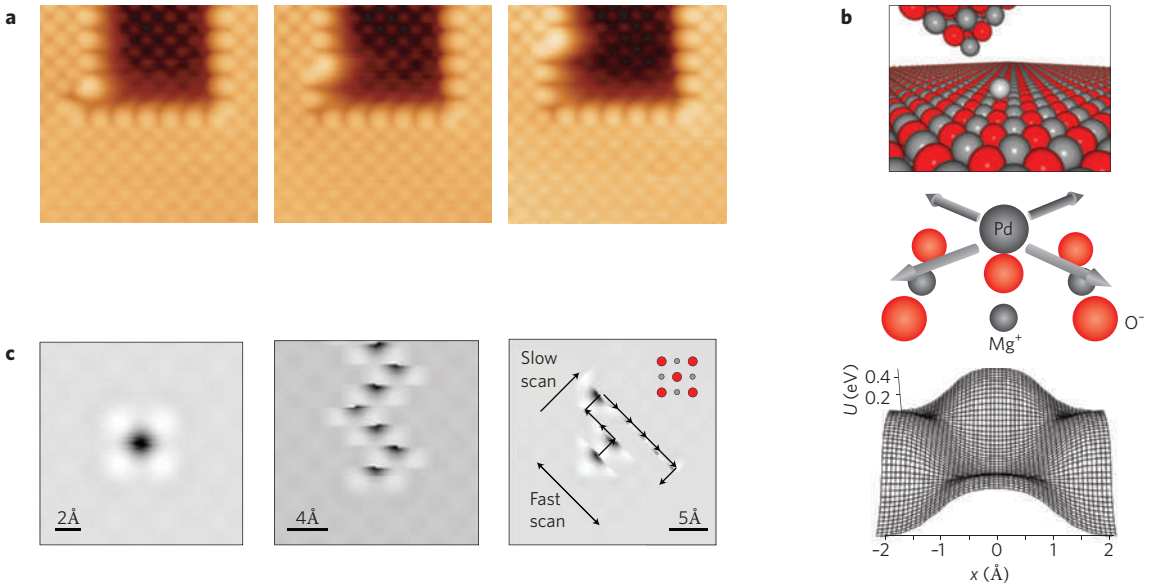

Figure 3 | Atomic-scale manipulation at surfaces of insulating bulk materials. a, Manipulation of atoms of a kink site at the step edge of a KBr(100) surface performed by applying the same protocol used for the manipulation process shown in Fig. 1b. **b**, Representation of a Pd atom adsorbed on top of a MgO(100) surface, probed with a MgO-terminated tip (red and dark grey spheres correspond to O^- and Mg^+ ions, respectively). The lower panel shows the simulated energy barriers (U) and minimum energy paths for the movement of the Pd atom, where x denotes interatomic spacing between ions. **c**, Simulated constant-height-scan AFM images during the manipulation of the Pd atom[69]: left, atom stably adsorbed on top of an oxygen atom; centre, tip-induced hopping of the Pd atom by raster scanning of the AFM tip; right, manipulation of the Pd atom along two crystallographic directions of the MgO(100) surface respectively aligned with the tip fast- and slow-scan directions.

Further experiments and atomistic simulations have shed some light on the complex mechanism of the lateral-interchange atomic manipulation process[33,53–55]. The above-mentioned Sn–Ge system behaves similarly to substitutional Pb atoms embedded in the plane of the Ge(111)-c(2 × 8) surface, where spontaneous in-plane concerted-interchange diffusion between Pb and Ge atoms has been observed at temperatures slightly above room temperature[46]. Similar diffusion behaviour — but at higher temperatures — is also expected for all the different surfaces shown in Fig. 1. The presence of the AFM tip, however, locally modifies the surface-potential landscape, lowering the natural energy barriers for the in-plane interchange diffusion below a limit that allows thermally activated hopping at room temperature, which is assisted by the directionality imposed by the tip scan[33,53,54]. A comparison between the measured tip–surface short-range forces in atom manipulation experiments and results from first-principle calculations has enabled the reduction in the energy barriers to be quantified[54]. Here, the interaction with the AFM tip produces a double effect: first, weakening the binding of the surface atoms with the underlying atomic plane; and second, stabilizing metastable surface adsorption positions along the manipulation path by offering an extra bond with the foremost atom of the tip[54]. A directionality imposed by scanning from one atom towards the other, lifting the AFM tip up on the way back, is therefore required to break the symmetry and to induce a preferential displacement of the atoms.

It is plausible that a similar situation occurs in the direction perpendicular to the surface: by gradually approaching the AFM tip towards the surface, there would be a threshold interaction at which the energy barriers for the interchange of the closest tip and surface atoms will be reduced below a value that would allow a thermally activated interchange at room temperature. This vertical interchange manipulation mechanism has been identified and recently reported by Sugimoto and co-workers[56] on the Sn/Si(111)-($\sqrt{3} \times \sqrt{3}$)R30° surface — a single atomic layer of Sn grown on top of a Si(111) substrate. In this surface, randomly distributed Si defects (protrusions with diminished contrast in Fig. 2) can be found in the plane of the Sn layer. These authors have demonstrated successive alternate deposition of Sn and Si atoms coming from the AFM tip over the same atomic surface location by gently exploring the repulsive part of the tip–surface short-range interaction (Fig. 2a), involving complex multi-atom contacts (Fig. 2e). This procedure allows them to 'write with atoms' — that is, to create atomic patterns by successively depositing Si atoms (Fig. 2b) and removing markers by sequentially depositing Sn (Fig. 2c). Although the process for producing tips that allow both writing and erasing is not fully controlled[56], reproducibility of vertical-interchange atom manipulation processes led the authors to create the atomic design shown in Fig. 2d, in a record time.

The creation of these artificial structures at room temperature illustrates the significant potential of the AFM for engineering complex atomic patterns of strongly bound atoms at heterogeneous semiconductor surfaces.

Manipulation at surfaces of bulk insulators

One of the most promising applications of the AFM is to explore and interact with surfaces of insulating bulk materials at the atomic scale. Although progress has been made on imaging surfaces of bulk insulators with atomic resolution[57–61], the capabilities of the AFM to manipulate atoms and molecules on such surfaces have barely been explored. This is because of the small adsorption energies of metallic adsorbates and some molecules on insulating surfaces[62]. Therefore one is compelled to perform controlled atomic manipulations at cryogenic temperatures[63,64]. Nonetheless, some hints of the potential of the AFM for atomic-scale manipulations at surfaces of bulk insulators have recently been obtained.

Hirth and co-workers[65] reported tip-induced displacements of atom-size defects on a CaF_2(111) surface at room temperature. Almost simultaneously, Nishi *et al.*[66] reported similar results on the KCl(100) surface. In these studies, the defects were dragged by the AFM tip along the slow-scan direction at given threshold tip–surface distances, following certain surface crystallographic directions. Another example of atomic-scale manipulation on insulating

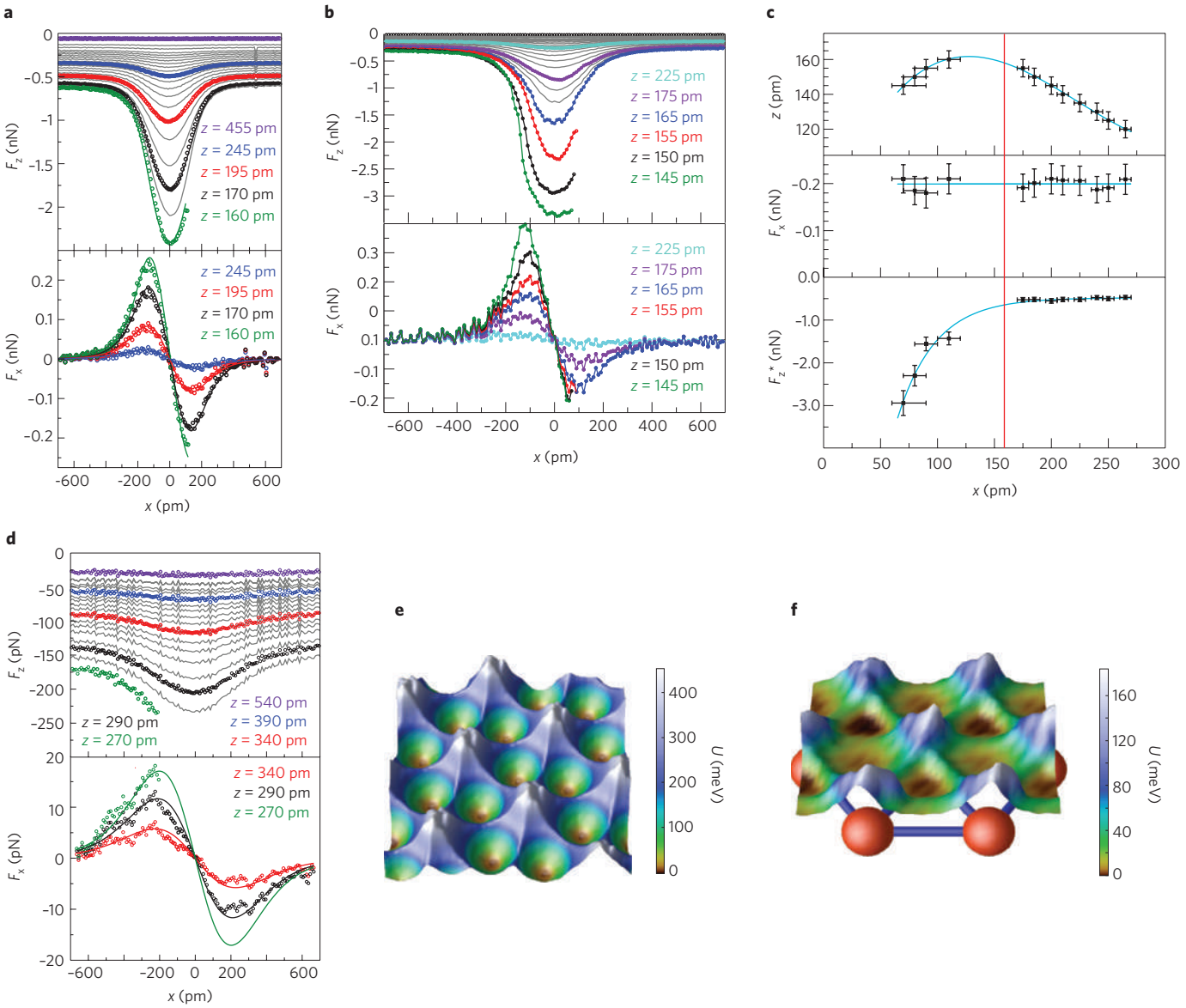

Figure 4 | Tip–surface interaction forces and potential maps during atom manipulation[76]. **a**, Vertical (F_Z) and lateral (F_X) forces — measured over a Co atom adsorbed on a Pt(111) surface at several tip–surface separations (z), until reaching z = 160 pm — that lead to the atom manipulation. A discontinuity defines the corresponding threshold forces required to move the atom. **b**, Measured threshold forces for the manipulation of the Co atom at closer z values than in **a**. **c**, Summary of the measured threshold forces to move a Co atom on Pt(111). Here, the threshold short-range vertical force (F_Z*) is obtained by subtracting the background long-range forces (in these experiments, the flat force level registered at the most distant lateral position from the Co atom) to F_Z. In **a**, **b** and **c**, the Co atom was located at the origin of the tip lateral position axis (x). In **c** the next stable empty adsorption site is marked by the red vertical line. The forces on the left of this line correspond to threshold values when the AFM tip approaches the atom, passes over it, and descends towards the surface on the way to the next neighbouring adsorption site; the forces on the right correspond to threshold values when the tip approaches the atom beyond the empty neighbouring adsorption site. The threshold lateral force remains constant, independently of the tip–sample separation, vertical force exerted over the atom and direction of the tip approaching it. **d**, F_Z and F_X measurements during the manipulation of a Co atom on a Cu(111) surface. **e**,**f**, Tip–adsorbate–surface interaction potential (U) maps for the manipulation of a Co atom on Pt(111) and on Cu(111), respectively.

surfaces is the manipulation of the atoms of a kink site at the step edge of a KBr(100) surface (Fig. 3a), at a tip–surface temperature of 80 K. Here, aiming for a higher degree of control, the authors used a similar protocol as for the manipulation shown in Fig. 1b, performing line scans over the kink site in a direction perpendicular to the step line, progressively increasing the tip–surface interaction force. As a result, the kink site was forced to migrate along the step edge in several manipulation events (Fig. 3a).

In contrast to the still scarce amount of experimental information on atomic manipulation at surfaces of bulk insulators, there is a wealth of theoretical predictions from atomistic simulations. For instance, Trevethan *et al.* and Watkins *et al.* have studied the possibility of manipulating atomic vacancies at the MgO(100) surface[67,68] by inducing successive jumps of neighbouring oxygen atoms into the vacancy with the AFM tip. Particularly inspiring are the predictions of the lateral manipulation of a single Pd adatom adsorbed over a MgO(100) surface, reported by Trevethan and co-workers[69]. These authors use a multi-scale modelling approach that allows them to: (1) determine the energy barriers for the adsorbate movement in three dimensions and characterize the minimum energy path for the atom displacement (Fig. 3b); (2) characterize the dynamic evolution of the system, including the tip oscillation

and the variation of the energy barriers according to the lateral displacement of the tip; and (3) simulate images of the tip-induced hopping of the Pd atom (Fig. 3c), providing all the corresponding signals intrinsic to the AFM during the manipulation[69]. All this information allows them to predict an optimum manipulation protocol and maps of the probability distribution for successful manipulation along the different minimum energy paths at different temperatures[69]. Interestingly, the basic mechanism for both the manipulation of an atomic vacancy and a Pb adsorbate at the MgO(100) surface relies on the reduction of the energy barriers for the natural diffusion of the involved atoms by the interaction with the AFM tip[67–69].

Force quantification during atom manipulation

As it was suggested by Stroscio and Eigler in their review on atomic and molecular manipulation with the STM, an AFM could be used to measure the tip–adsorbate force during lateral-manipulation events, and to map the potential between the adsorbate and the surface[43]. The technique to do so is force spectroscopy, which nowadays enables us to precisely quantify the tip–surface interaction force with subatomic spatial resolution by mapping the variation of the cantilever resonant frequency in one[70–74], two[59,75] or three[76,77] dimensions. These changes in the resonant frequency are converted into the tip–surface interaction force[78–80] through a mathematical transformation[80–83], and integration of these forces over the explored tip–surface distance range results in the estimation of the corresponding interaction potential.

The first experimental estimation of the force required to manipulate an atom was reported by Sugimoto and co-workers during the room-temperature manipulation of intrinsic atoms of the Si(111)-(7 × 7) surface in the presence of an atomic vacancy[54]. By combining manipulation with force spectroscopy experiments, these authors reported that a force of approximately −0.5 nN is needed to move a Si atom along the dimer rows and across the half unit cell of the (7 × 7) reconstruction. This force was estimated by correlating the threshold resonant frequency set-point required to manipulate the atom with the corresponding vertical force measured over a static Si adatom, and thus it cannot be considered a proper measurement of the tip–surface interaction forces during atom manipulation.

The most accurate determination of the threshold forces required to manipulate atoms and molecules at metallic surfaces was accomplished by Ternes and co-workers[76]. Using the qPlus sensor[84,85], these authors were able to measure the tunnelling current, as well as the vertical and lateral forces during the lateral manipulation of a Co atom on a Pt(111) and a Cu(111) surface, and compare the behaviour of these observables with the ones obtained from the manipulation of a CO molecule on a Cu(111) surface.

Figures 4a and b show the vertical (F_Z) and lateral (F_X) forces measured during the manipulation of a Co atom across two neighbouring threefold hollow sites of the Pt(111) surface, produced by executing constant-height line scans over the Co atom at successive smaller tip–surface separations[76,86]. A discontinuity in the curves defines the corresponding threshold forces required to move the atom. Astonishingly, the measurement of these forces at tip–surface distances smaller than 160 pm (the maximum separation leading to the atom manipulation), reveals that while the vertical threshold force exerted over the Co atom almost doubles its value, the corresponding lateral forces remain steady, as shown in Fig. 4b. A systematic quantification of the forces required to manipulate the Co atom when the tip is approaching from the far right and far left end of the line scan at different tip–surface separations confirms the invariability of the lateral threshold force, as it is summarized in Fig. 4c. These results point towards the short-range lateral force exerted by the tip apex as being key for the manipulation of individual metal atoms on metallic surfaces at cryogenic temperatures[76]. Furthermore, the invariability of this lateral force with the tip–surface separation contrasts with the energy-barrier reduction mechanism reported in the case of atom manipulation with an AFM on semiconductors and insulating materials summarized in the preceding sections.

This constant behaviour of the lateral threshold force enabled Ternes and co-workers to compare the lateral forces required to manipulate the same atomic species over a Cu(111) surface[76]. Surprisingly, the lateral threshold forces to move a Co atom on a Cu(111) surface were almost one order of magnitude lower (see Fig. 4d) than in the Pt(111) case, even when the surface structure and the adsorption site of the Co atom are equivalent in both surfaces. These results highlight the relevance of the chemical interaction of the adsorbate with the substrate in atom manipulation experiments and, more importantly, set the basis for the quantification of friction at the single-atom scale[76].

By combining three-dimensional maps of the tip–surface interaction force at two different separation regimes (above and below the threshold distance for atom manipulation), Ternes and co-workers also calculated the tip–adatom–surface interaction potential[76] for the manipulation of a Co atom on Pt(111) and on Cu(111) (Fig. 4e,f). These potential maps provide experimental evidence of the relative adsorption stability of the atom on the different surface binding sites available. Unexpectedly, the energy barriers for the transition of the Co atom between two neighbouring threefold hollow adsorption sites obtained from these maps match the corresponding natural-diffusion energy barriers (in absence of the AFM tip) obtained from atomistic simulations[76]; a remarkable result that requires further consideration, and that may present a new way of quantifying diffusion energy barriers of adsorbates on surfaces.

Concluding remarks and outlook

In the preceding sections we have shown that the AFM can be applied to purposefully create complex designs at semiconductor surfaces one atom at a time, to perform atomic manipulations on surfaces of insulating bulk materials, and to measure the forces involved in the manipulation of atoms and molecules with the possibility of quantifying friction at the atomic scale and characterizing diffusion energy barriers. Despite all this recent progress, atomic and molecular manipulation with the AFM is still at its inception.

There are plenty of promising applications to investigate with the AFM, in which atomic-scale manipulation will surely be a pivotal tool. Manipulation of small molecules with the AFM has barely been studied[87–90], and manipulation of atoms and molecules on surfaces of bulk insulators is an open avenue to be explored. It may be particularly promising to combine the atom manipulation capabilities of the AFM with recent advances for the characterization of magnetic interactions[91–93], spin detection[94,95], characterization of the charge state of individual adatoms[96], intramolecular chemical resolution[97] and single-atom chemical identification[98].

In many of these applications involving atomic manipulation with the AFM, the prospect of simultaneously measuring and correlating tunnelling currents — when electric conduction is possible — and tip–surface interaction forces is most promising[76]. As the most basic feature, this approach will allow us to identify structures invisible for the STM but visible for the AFM, and vice versa[99]. Nowadays, it is possible to simultaneously measure tunnelling currents and tip–surface interaction forces at atomic scale with AFMs based on commercial silicon cantilevers[99–101], as well as with notable implementations such as the qPlus sensor[84,85] or the KolibriSensor[102,103]. These new sensors are based on piezoelectric detection, and have a high-resolution profile with relative instrumental simplicity; characteristics that make them very attractive

for performing simultaneous current and force measurements in extreme environments such as milli-Kelvin temperatures and high-magnetic fields. Hopefully, with the use of these implementations, the variety of systems to be explored and the number of groups working on atomic manipulation with the AFM will increase over the coming years, so that exciting discoveries and formidable technological achievements at the nanoscale will emerge.

References

1. Binnig, G., Rohrer, H., Gerber, C. & Weibel, E. Surface studies by scanning tunneling microscopy. *Phys. Rev. Lett.* **49,** 57–61 (1982).
2. Eigler, D. M. & Schweizer, E. K. Positioning single atoms with a scanning tunnelling microscope. *Nature* **344,** 524–526 (1990).
3. Lyo, I.-W. & Avouris, P. Field-induced nanometer- to atomic-scale manipulation of silicon surfaces with the STM. *Science* **253,** 173–176 (1991).
4. Eigler, D. M., Lutz, C. P. & Rudger, W. E. An atomic switch realized with the scanning tunnelling microscope. *Nature* **352,** 600–603 (1991).
5. Terabe, K., Hasegawa, T., Nakayama, T. & Aono, M. Quantized conductance atomic switch. *Nature* **433,** 47–50 (2005).
6. Nilius, N., Wallis, T. M. & Ho, W. Development of one-dimensional band structure in artificial gold chains. *Science* **297,** 1853–1856 (2002).
7. Nazin, G. V., Qiu, X. H. & Ho, W. Visualization and spectroscopy of a metal-molecule-metal bridge. *Science* **302,** 77–81 (2003).
8. Repp, J., Meyer, G., Paavilainen, S., Olsson, F. E. & Persson, M. Imaging bond formation between a gold atom and pentacene on an insulating surface. *Science* **312,** 1196–1199 (2006).
9. Lafferentz, L. *et al.* Conductance of a single conjugated polymer as a continuous function of its length. *Science* **323,** 1193–1197 (2009).
10. Heinrich, A. J., Lutz, C. P., Gupta, J. A. & Eigler, D. M. Molecule cascades. *Science* **298,** 1381–1387 (2002).
11. Crommie, M. F., Lutz, C. P. & Eigler, D. M. Confinement of electrons to quantum corrals on a metal surface. *Science* **262,** 218–220 (1993).
12. Heller, E. J., Crommie, M. F., Lutz, C. P. & Eigler, D. M. Scattering and adsorption of surface electron waves in quantum corrals. *Nature* **369,** 464–466 (1994).
13. Manoharan, H., Lutz, C. P. & Eigler, D. M. Quantum mirages formed by coherent projection of electronic structure. *Nature* **403,** 512–515 (2000).
14. Moon, C. R., Mattos, L. S., Foster, B. K., Zeltzer, G. & Manoharan, H. C. Quantum holographic encoding in a two-dimensional electron gas. *Nature Nanotech.* **4,** 167–172 (2009).
15. Kitchen, D., Richardella, A., Tang, J.-M., Flatté, M. E. & Yazdani, A. Atom-by-atom substitution of Mn in GaAs and visualization of their hole-mediated interactions. *Nature* **442,** 436–439 (2006).
16. Yamachika, R., Grobis, M., Wachowiak, A. & Crommie, M. F. Controlled atomic doping of a single C_{60} molecule. *Science* **304,** 281–284 (2004).
17. Hla, S.-W., Bartels, L., Meyer, G. & Rieder, K.-H. Inducing all steps of a chemical reaction with the scanning tunneling microscope tip: Towards single molecule engineering. *Phys. Rev. Lett.* **85,** 2777–2780 (2000).
18. Jung, T. A., Schlittler, R. R., Gimzewski, J. K., Tang, H. & Joachim, C. Controlled room temperature positioning of individual molecules: Molecular flexure and motion. *Science* **271,** 181–184 (1996).
19. Gimzewski, J. K. *et al.* Rotation of a single molecule within a supramolecular bearing. *Science* **281,** 531–533 (1998).
20. Stipe, B. C. & Ho, W. Inducing and viewing the rotational motion of a single molecule. *Science* **279,** 1907–1909 (1998).
21. Komeda, T., Kim, Y., Kawai, M., Persson, B. N. J. & Ueba, H. Lateral hopping of molecules induced by excitation of internal vibration mode. *Science* **295,** 2055–2058 (2002).
22. Pascual, J. I., Lorente, N., Song, Z., Conrad, H. & Rust, H.-P. Selectivity in vibrationally mediated single-molecule chemistry. *Nature* **423,** 525–528 (2003).
23. Lee, H. J. & Ho, W. Single-bond formation and characterization with a scanning tunneling microscope. *Science* **286,** 1719–1722 (1999).
24. Chen, W., Jamneala, T., Madhavan, V. & Crommie, M. F. Disappearance of the Kondo resonance for atomically fabricated cobalt dimers. *Phys. Rev. B* **60,** R8529 (1999).
25. Hirjibehedin, C. F., Lutz, C. P. & Heinrich, A. J. Spin coupling in engineered atomic structures. *Science* **312,** 1021–1023 (2006).
26. Giessibl, F. J. & Quate, C. F. Exploring the nanoworld with atomic force microscopy. *Physics Today* **59,** 44–50 (2006).
27. Giessibl, F. J. Advances in atomic force microscopy. *Rev. Mod. Phys.* **75,** 949–983 (2003).
28. García, R. & Pérez, R. Dynamic atomic force microscopy methods. *Surf. Sci. Rep.* **47,** 197–301 (2002).
29. Binnig, G., Quate, C. F. & Gerber, C. Atomic force microscope. *Phys. Rev. Lett.* **56,** 930–933 (1986).
30. Gerber, C. & Lang, H. How the doors to the nanoworld were opened. *Nature Nanotech.* **1,** 3–5 (2006).
31. Binnig, G., Rohrer, H., Gerber, C. & Weibel, E. 7 × 7 reconstruction on Si(111) resolved in real space. *Phys. Rev. Lett.* **50,** 120–123 (1983).
32. Giessibl, F. J. Atomic resolution of the silicon(111)-(7 × 7) surface by atomic force microscopy. *Science* **267,** 68–71 (1995).
33. Sugimoto, Y. *et al.* Atom inlays performed at room temperature using atomic force microscopy. *Nature Mater.* **4,** 156–159 (2005).
34. Binnig, G. & Rohrer, H. In touch with atoms. *Rev. Mod. Phys.* **71,** S324 (1999).
35. Pérez, R., Payne, M., Štich, I. & Terakura, K. Role of covalent tip-surface interactions in noncontact atomic force microscopy. *Phys. Rev. Lett.* **78,** 678–681 (1997).
36. Livshits, A. I., Shluger, A. L., Rohl, A. L. & Foster, A. S. Model of noncontact scanning force microscopy on ionic surfaces. *Phys. Rev. B* **59,** 2436–2448 (1999).
37. Dieška, P., Štich, I. & Pérez, R. Covalent and reversible short-range electrostatic imaging in noncontact atomic force microscopy. *Phys. Rev. Lett.* **91,** 216401 (2003).
38. Hölscher, H., Allers, W., Schwarz, U. D., Schwarz, A. & Wiesendanger, R. Simulation of NC-AFM images of xenon(111). *Appl. Phys. A* **72,** S35–S38 (2001).
39. Albrecht, T. R., Grütter, P., Horne, D. & Rugar, D. Frequency modulation detection using high-Q cantilevers for enhanced force microscope sensitivity. *J. Appl. Phys.* **69,** 668–673 (1991).
40. Guggisberg, M. *et al.* Separation of interactions by noncontact force microscopy. *Phys. Rev. B* **61,** 11151–11155 (2000).
41. Giessibl, F. J., Hembacher, S., Herz, M., Schiller, C. & Mannhart, J. Stability considerations and implementation of cantilevers allowing dynamic force microscopy with optimal resolution: the qPlus sensor. *Nanotechnology* **15,** S79–S86 (2004).
42. Hosoki, S., Hosaka, S. & Hasegawa, T. Surface modification of MoS_2 using an STM. *Appl. Surf. Sci.* **60–61,** 643–647 (1992).
43. Stroscio, J. A. & Eigler, D. M. Atomic and molecular manipulation with the scanning tunneling microscope. *Science* **254,** 1319–1326 (1991).
44. Bartels, L., Meyer, G. & Rieder, K.-H. Basic steps of lateral manipulation of single atoms and diatomic clusters with a scanning tunneling microscope tip. *Phys. Rev. Lett.* **79,** 697–700 (1997).
45. Oyabu, N., Custance, O., Yi, I., Sugawara, Y. & Morita, S. Mechanical vertical manipulation of selected single atoms by soft nanoindentation using near contact atomic force microscopy. *Phys. Rev. Lett.* **90,** 176102 (2003).
46. Oyabu, N., Sugimoto, Y., Abe, M., Custance, O. & Morita, S. Lateral manipulation of single atoms at semiconductor surfaces using atomic force microscopy. *Nanotechnology* **16,** S112–S117 (2005).
47. Brihuega, I., Custance, O. & Gómez-Rodríguez, J. M. Surface diffusion of single vacancies on Ge(111)-c(2 × 8) studied by variable temperature scanning tunneling microscopy. *Phys. Rev. B* **70,** 165410 (2004).
48. Pizzagalli, L. & Baratoff, A. Theory of single atom manipulation with a scanning probe tip: Force signatures, constant-height, and constant-force scans. *Phys. Rev. B* **68,** 115427 (2003).
49. Dieška, P., Štich, I. & Pérez, R. Nanomanipulation using only mechanical energy. *Phys. Rev. Lett.* **95,** 126103 (2005).
50. Meyer, G. *et al.* Manipulation of atoms and molecules with the low-temperature scanning tunneling microscope. *Jpn. J. Appl. Phys.* **40,** 4409–4413 (2001).
51. Cuberes, M. T., Schlittler, R. R. & Gimzewski, J. K. Room-temperature repositioning of individual C_{60} molecules at Cu steps: Operation of a molecular counting device. *Appl. Phys. Lett.* **69,** 3016–3018 (1996).
52. Sugimoto, Y., Custance, O., Abe, M. & Morita, S. Site-specific force spectroscopy and atom interchange manipulation at room temperature. *e-J. Surf. Sci. Nanotech.* **4,** 376–383 (2006).
53. Sugimoto, Y., Miki, K., Abe, M. & Morita, S. Statistics of lateral atom manipulation by atomic force microscopy at room temperature. *Phys. Rev. B* **78,** 205305 (2008).
54. Sugimoto, Y. *et al.* Mechanism for room-temperature single-atom lateral manipulations on semiconductors using dynamic force microscopy. *Phys. Rev. Lett.* **98,** 106104 (2007).
55. Dieška, P. & Štich, I. Nanoengineering with dynamic atomic force microscopy: Lateral interchange of adatoms on a Ge(111)-c(2 × 8) surface. *Phys. Rev. B* **79,** 125431 (2009).
56. Sugimoto, Y. *et al.* Complex patterning by vertical interchange atom manipulation using atomic force microscopy. *Science* **322,** 413–417 (2008).
57. Bammerlin, M. *et al.* Dynamic SFM with true atomic resolution on alkali halide surfaces. *Appl. Phys. A* **66,** S293–S294 (1998).
58. Reichling, M. & Barth, C. Scanning force imaging of atomic size defects on the CaF_2(111) surface. *Phys. Rev. Lett.* **83,** 768–771 (1999).
59. Hölscher, H., Langkat, S. M., Schwarz, A. & Wiesendanger, R. Measurement of three dimensional force fields with atomic resolution using dynamic force spectroscopy. *Appl. Phys. Lett.* **81,** 4428–4430 (2002).
60. Barth, C. & Henry, C. Atomic resolution imaging of the (001) surface of UHV cleaved MgO by dynamic scanning force microscopy. *Phys. Rev. Lett.* **91,** 196102 (2003).

61. Torbrügge, S., Reichling, M., Ishiyama, A., Morita, S. & Custance, O. Evidence of subsurface oxygen vacancy ordering on reduced CeO_2(111). *Phys. Rev. Lett.* **99,** 056101 (2007).
62. Hakala, M. H., Pakarinen, O. H. & Foster, A. S. First-principles study of adsorption, diffusion, and charge stability of metal adatoms on alkali halide surfaces. *Phys. Rev. B* **78,** 045418 (2008).
63. Repp, J., Meyer, G., Olsson, F. E. & Persson, M. Controlling the charge state of individual gold adatoms. *Science* **305,** 493–495 (2004).
64. Heinrich, A. J., Gupta, J. A., Lutz, C. P. & Eigler, D. M. Single-atom spin-flip spectroscopy. *Science* **306,** 466–469 (2004).
65. Hirth, S., Ostendorf, F. & Reichling, M. Lateral manipulation of atomic size defects on the CaF_2(111) surface. *Nanotechnology* **17,** S148–S154 (2006).
66. Nishi, R., Miyagawa, D., Seino, Y., Yi, I. & Morita, S. Non-contact atomic force microscopy study of atomic manipulation on an insulator surface by nanoindentation. *Nanotechnology* **17,** S142–S147 (2006).
67. Trevethan, T., Watkins, M., Kantorovich, L. N. & Shluger, A. L. Controlled manipulation of atoms in insulating surfaces with the virtual atomic force microscope. *Phys. Rev. Lett.* **98,** 028101 (2007).
68. Watkins, M. B. & Shluger, A. L. Manipulation of defects on oxide surfaces via barrier reduction induced by atomic force microscope tips. *Phys. Rev. B* **73,** 245435 (2006).
69. Trevethan, T., Kantorovich, L., Polesel-Maris, J., Gauthier, S. & Shluger, A. Multiscale model of the manipulation of single atoms on insulating surfaces using an atomic force microscope tip. *Phys. Rev. B* **76,** 085414 (2007).
70. Lantz, M. A. *et al.* Quantitative measurement of short-range chemical bonding forces. *Science* **291,** 2580–2583 (2001).
71. Hoffmann, R., Kantorovich, L. N., Baratoff, A., Hug, H. J. & Güntherodt, H.-J. Sublattice identification in scanning force microscopy on alkali halide surfaces. *Phys. Rev. Lett.* **92,** 146103 (2004).
72. Oyabu, N. *et al.* Single atomic contact adhesion and dissipation in dynamic force microscopy. *Phys. Rev. Lett.* **96,** 106101 (2006).
73. Abe, M., Sugimoto, Y., Custance, O. & Morita, S. Room-temperature reproducible spatial force spectroscopy using atom-tracking technique. *Appl. Phys. Lett.* **87,** 173503 (2005).
74. Sugimoto, Y., Innami, S., Abe, M., Custance, O. & Morita, S. Dynamic force spectroscopy using cantilever higher flexural modes. *Appl. Phys. Lett.* **91,** 093120 (2007).
75. Schirmeisen, A., Weiner, D. & Fuchs, H. Single-atom contact mechanics: From atomic scale energy barrier to mechanical relaxation hysteresis. *Phys. Rev. Lett.* **97,** 136101 (2006).
76. Ternes, M., Lutz, C. P., Hirjibehedin, C. F., Giessibl, F. J. & Heinrich, A. J. The force needed to move an atom on a surface. *Science* **319,** 1066–1069 (2008).
77. Albers, B. J. *et al.* Three-dimensional imaging of short-range chemical forces with picometre resolution. *Nature Nanotech.* **4,** 307–310 (2009).
78. Giessibl, F. J. Forces and frequency shifts in atomic-resolution dynamic-force microscopy. *Phys. Rev. B* **56,** 16010–16015 (1997).
79. Hölscher, H. *et al.* Measurement of conservative and dissipative tip-sample interaction forces with a dynamic force microscope using the frequency modulation technique. *Phys. Rev. B* **64,** 075402 (2001).
80. Dürig, U. Extracting interaction forces and complementary observables in dynamic probe microscopy. *Appl. Phys. Lett.* **76,** 1203–1205 (2000).
81. Gotsmann, B., Anczykowski, B., Seidel, C. & Fuchs, H. Determination of tip-sample interaction forces from measured dynamic force spectroscopy curves. *Appl. Surf. Sci.* **140,** 314–319 (1999).
82. Giessibl, F. J. A direct method to calculate tip-sample forces from frequency shifts in frequency-modulation atomic force microscopy. *Appl. Phys. Lett.* **78,** 123–125 (2001).
83. Sader, J. E. & Jarvis, S. P. Accurate formulas for interaction force and energy in frequency modulation force spectroscopy. *Appl. Phys. Lett.* **84,** 1801–1803 (2004).
84. Giessibl, F. J. High-speed force sensor for force microscopy and profilometry utilizing a quartz tuning fork. *Appl. Phys. Lett.* **73,** 3956–3958 (1998).
85. Giessibl, F. J. Atomic resolution on Si(111)-(7 × 7) by noncontact atomic force microscopy with a force sensor based on a quartz tuning fork. *Appl. Phys. Lett.* **76,** 1470–1472 (2000).
86. Custance, O. & Morita, S. How to move an atom. *Science* **319,** 1051–1052 (2008).
87. Mativetsky, J., Burke, S. A., Hoffmann, R., Sun, Y. & Grutter, P. Molecular resolution imaging of C_{60} on Au(111) by non-contact atomic force microscopy. *Nanotechnology* **15,** S40–S43 (2004).
88. Atodiresei, N., Caciuc, V., Blügel, S. & Hölscher, H. Manipulation of benzene on Cu(110) by dynamic force microscopy: An *ab initio* study. *Phys. Rev. B* **77,** 153408 (2008).
89. Glatzel, T., Zimmerli, L., Koch, S., Kawai, S. & Meyer, E. Molecular assemblies grown between metallic contacts on insulating surfaces. *Appl. Phys. Lett.* **94,** 063303 (2009).
90. Martsinovich, N. & Kantorovich, L. Modelling the manipulation of C_{60} on the Si(001) surface performed with NC-AFM. *Nanotechnology* **20,** 135706 (2009).
91. Kaiser, U., Schwarz, A. & Wiesendanger, R. Magnetic exchange force microscopy with atomic resolution. *Nature* **446,** 522–525 (2007).
92. Lazo, C., Caciuc, V., Hölscher, H. & Heinze, S. Role of tip size, orientation, and structural relaxations in first-principles studies of magnetic exchange force microscopy and spin-polarized scanning tunneling microscopy. *Phys. Rev. B* **78,** 214416 (2008).
93. Schmidt, R. *et al.* Probing the magnetic exchange forces of iron on the atomic scale. *Nano Lett.* **9,** 200–204 (2009).
94. Rugar, D., Budakian, R., Mamin, H. J. & Chui, B. W. Single spin detection by magnetic resonance force microscopy. *Nature* **430,** 329–332 (2004).
95. Degen, C. L., Poggio, M., Mamin, H. J., Rettner, C. T. & Rugar, D. Nanoscale magnetic resonance imaging. *Proc. Natl Acad. Sci. USA* **106,** 1313–1317 (2009).
96. Gross, L. *et al.* Measuring the charge state of an adatom with noncontact atomic force microscopy. *Science* **324,** 1428–1431 (2009).
97. Gross, L., Mohn, F., Moll, N., Liljeroth, P. & Meyer, G. The chemical structure of a molecule resolved by atomic force microscopy. *Science* **325,** 1110–1114 (2009).
98. Sugimoto, Y. *et al.* Chemical identification of individual surface atoms by atomic force microscopy. *Nature* **445,** 64–67 (2007).
99. Enevoldsen, G. H. *et al.* Imaging of the hydrogen subsurface site in rutile TiO_2. *Phys. Rev. Lett.* **102,** 136103 (2009).
100. Özer, H. Ö., O'Brien, S. J. & Pethica, J. B. Local force gradients on Si(111) during simultaneous scanning tunneling/atomic force microscopy. *Appl. Phys. Lett.* **90,** 133110 (2007).
101. Sawada, D., Sugimoto, Y., Morita, K., Abe, M. & Morita, S. Simultaneous measurement of force and tunneling current at room temperature. *Appl. Phys. Lett.* **94,** 173117 (2009).
102. Clauss, W., Zhang, J., Bergeron, D. J. & Johnson, A. T. Application and calibration of a quartz needle sensor for high resolution scanning force microscopy. *J. Vac. Sci. Technol. B* **17,** 1309–1312 (1999).
103. An, T. *et al.* Atomically resolved imaging by low-temperature frequency-modulation atomic force microscopy using a quartz length-extension resonator. *Rev. Sci. Instrum.* **79,** 033703 (2008).

Acknowledgements

The authors thank M. Ternes, A. Heinrich and T. Trevethan for providing graphic material. Work supported by Grants in Aid for Science Research from the Ministry of Education, Culture, Sports, Science and Technology of Japan, by the Ministerio de Ciencia e Innovación of Spain (MICINN, projects MAT2008-02929-NAN and MAT2008-02939-E) and by the Friction and Adhesion in Nanomechanical Systems (FANAS) Programme of the European Science Foundation under the Atomic Friction (AFRI) project.

Additional information

The authors declare no competing financial interests.